Electronic Supplementary Material (ESI) for Nanoscale.

Supplementary Information

Single molybdenum atom anchored on 2D Ti_2NO_2 MXene as a promising electrocatalyst for N_2 fixation

Yuwen Cheng,[a,b] Jianhong Dai,[a] Yan Song,[a,*] Yumin Zhang[b,*]

a School of Materials Science and Engineering, Harbin Institute of Technology at Weihai, 2 West Wenhua Road, Weihai, 264209, PR China

b National Key Laboratory of Science and Technology for National Defence on Advanced Composites in Special Environments, Harbin Institute of Technology, Harbin, 150001, PR China

*** Corresponding Authors**

E-mail: sy@hitwh.edu.cn (Y.S). E-mail: zhym@hit.edu.cn (Y.M.Z).

1. Reaction mechanisms of nitrogen reduction into ammonia

The reactions of each possible reduction mechanisms are taken into consideration, the reactions for NRR are as below:

Alternating:

$$*+N_2 \rightarrow *N\text{-}N \qquad \Delta G_1 \tag{S1}$$

$$*N\text{-}N+H^++e^- \rightarrow *N\text{-}NH \qquad \Delta G_2 \tag{S2}$$

$$*N\text{-}NH+H^++e^- \rightarrow *NH\text{-}NH \qquad \Delta G_3 \tag{S3}$$

$$*NH\text{-}NH+H^++e^- \rightarrow *NH\text{-}NH_2 \qquad \Delta G_4 \tag{S4}$$

$$*NH\text{-}NH_2+H^++e^- \rightarrow *NH_2\text{-}NH_2 \qquad \Delta G_5 \tag{S5}$$

$$*NH\text{-}NH_2+H^++e^- \rightarrow *NH_2+NH_3 \qquad \Delta G_6 \tag{S6}$$

$$*NH_2+H^++e^- \rightarrow *NH_3 \qquad \Delta G_7 \tag{S7}$$

$$*NH_3 \rightarrow *+NH_3 \qquad \Delta G_8 \tag{S8}$$

Distal:

$$*+N_2 \rightarrow *N\text{-}N \qquad \Delta G_1 \tag{S1}$$

$$*N\text{-}N+H^++e^- \rightarrow *N\text{-}NH \qquad \Delta G_2 \tag{S2}$$

$$*N\text{-}NH+H^++e^- \rightarrow *N\text{-}NH_2 \qquad \Delta G_9 \tag{S9}$$

$$*N\text{-}NH_2+H^++e^- \rightarrow *N+NH_3 \qquad \Delta G_{10} \tag{S10}$$

$$*N+H^++e^- \rightarrow *NH \qquad \Delta G_{11} \tag{S11}$$

$$*NH+H^++e^- \rightarrow *NH_2 \qquad \Delta G_{12} \tag{S12}$$

$$*NH_2+H^++e^- \rightarrow *NH_3 \qquad \Delta G_7 \tag{S7}$$

$$*NH_3 \rightarrow *+NH_3 \qquad \Delta G_8 \tag{S8}$$

Enzymatic:

$$*+N_2 \rightarrow *N\text{-}*N \qquad \Delta G_{13} \tag{S13}$$

$$*N\text{-}*N+H^++e^- \rightarrow *N\text{-}*NH \qquad \Delta G_{14} \tag{S14}$$

$$*N\text{-}*NH+H^++e^- \rightarrow *NH\text{-}*NH \qquad \Delta G_{15} \tag{S15}$$

$$*NH\text{-}*NH+H^++e^- \rightarrow *NH\text{-}*NH_2 \qquad \Delta G_{16} \tag{S16}$$

$$*NH\text{-}*NH_2+H^++e^- \rightarrow *NH_2\text{-}*NH_2 \qquad \Delta G_{17} \tag{S17}$$

$$*NH\text{-}*NH_2+H^++e^- \rightarrow *NH_2\text{-}*NH_3 \qquad \Delta G_{18} \tag{S18}$$

$$*NH_2\text{-}*NH_3+H^++e^- \rightarrow *NH_3+NH_3 \qquad \Delta G_{19} \tag{S19}$$

$$*NH_3 \rightarrow *+NH_3 \qquad \Delta G_8 \tag{S8}$$

Consecutive:

$$*+N_2 \rightarrow *N\text{-}*N \qquad \Delta G_{13} \tag{S13}$$

$$*N\text{-}*N+H^++e^- \rightarrow *N\text{-}*NH \qquad \Delta G_{14} \tag{S14}$$

$$*N\text{-}*NH+H^++e^- \rightarrow *N\text{-}*NH_2 \qquad \Delta G_{20} \tag{S20}$$

$$*N\text{-}*NH_2+H^++e^- \rightarrow *N+NH_3 \qquad \Delta G_{21} \tag{S21}$$

$$*N+H^++e^- \rightarrow *NH \qquad \Delta G_{11} \tag{S11}$$

$$*NH+H^++e^- \rightarrow *NH_2 \qquad \Delta G_{12} \tag{S12}$$

$$*NH_2+H^++e^- \rightarrow *NH_3 \qquad \Delta G_7 \tag{S7}$$

$$*NH_3 \rightarrow *+NH_3 \qquad \Delta G_8 \tag{S8}$$

For alternating mechanism, the protonation continuously occurs on two sides until formation of $*NH_2\text{-}NH_2$ species following $*N_2$ configuration and the first NH_3 released. The second NH_3 is generated following the $*NH_2$ and $*NH_3$. For distal mechanism, the protonation continuously occurs on one side until first NH_3 released, and then second NH_3 is released after the *N species hydrogenated into *NH, *NH_2 and *NH_3. For enzymatic mechanism, N_2 adsorption and forms the *N-*N configuration, the protonation continuously occurs on two sides until the formation of *NH_2-*NH_2 species and the NH_3 released successively. For consecutive mechanism, the protonation continuously occurs on one side, forming the *NH-*NH, *NH_2-*NH until first NH_3 released, and then second NH_3 is generated after the *N species hydrogenated into *NH, *NH_2 and *NH_3.

2. Figures and Tables

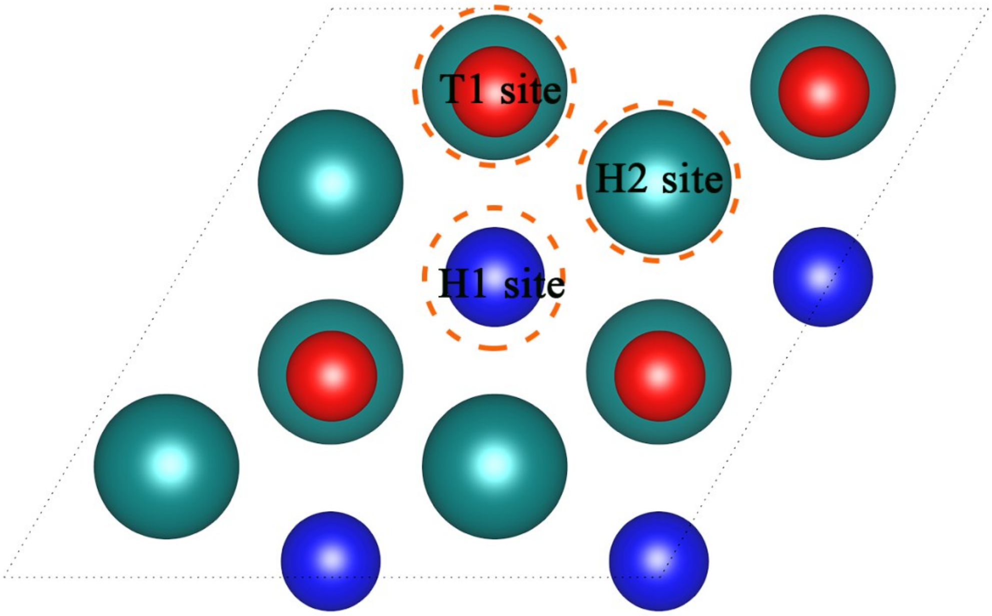

Figure S1. Schematic of possible sites of TM on M_2NO_2. The green, red, blue balls stand for M (Ti, V, and Cr) metal, O, and N atoms, respectively.

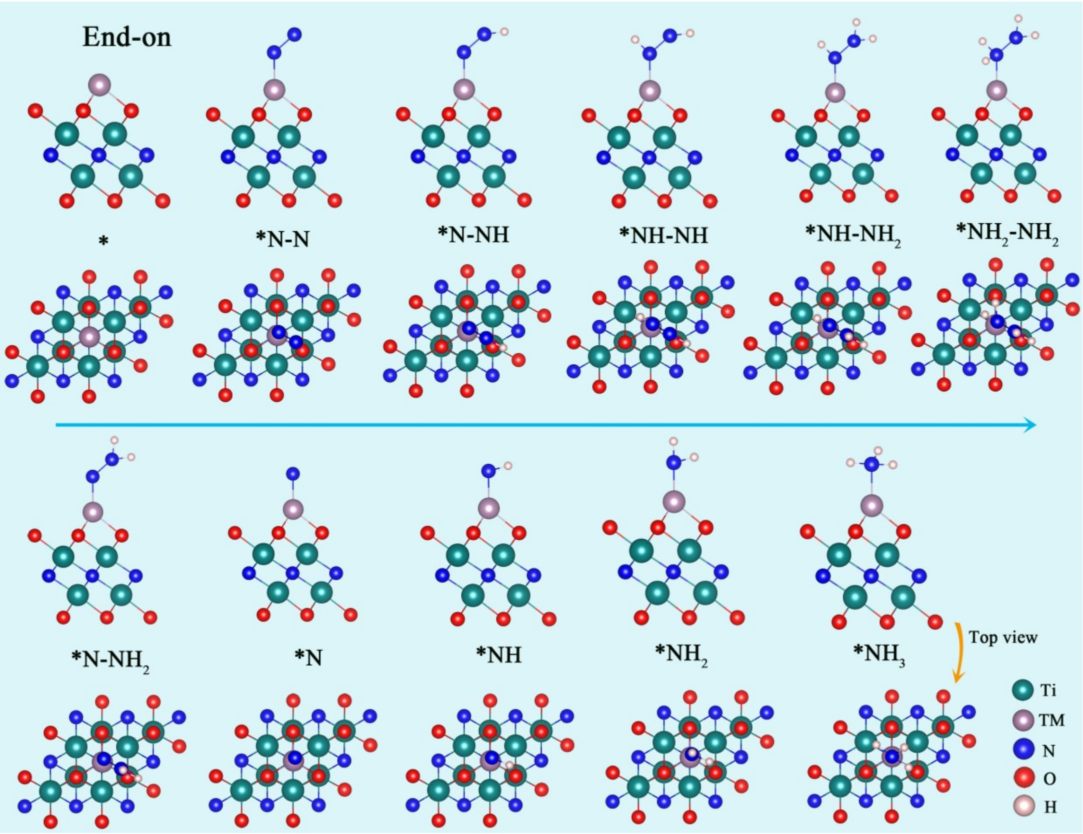

Figure S2. Schematic structures of intermediates of NRR on TM/Ti_2NO_2 surface for the end-on configuration via alternative and distal mechanisms.

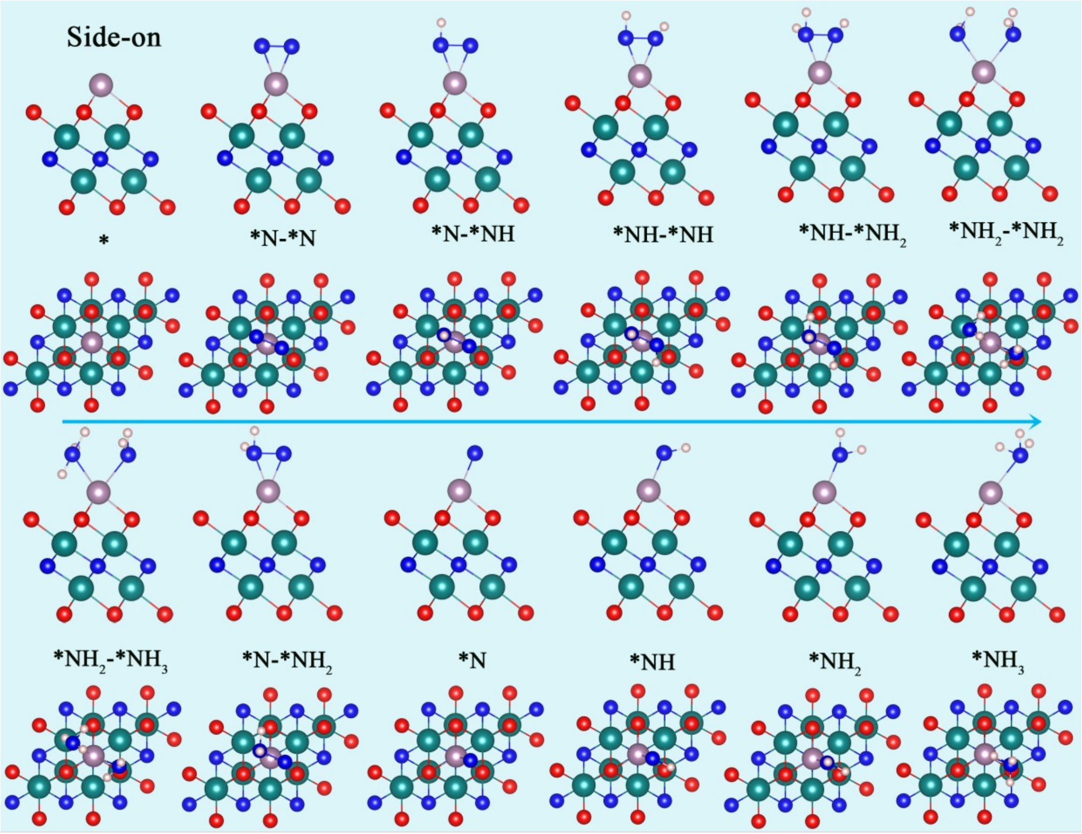

Figure S3. Schematic structures of intermediates of NRR on TM/Ti_2NO_2 surface for the side-on configuration via enzymatic and consecutive mechanisms.

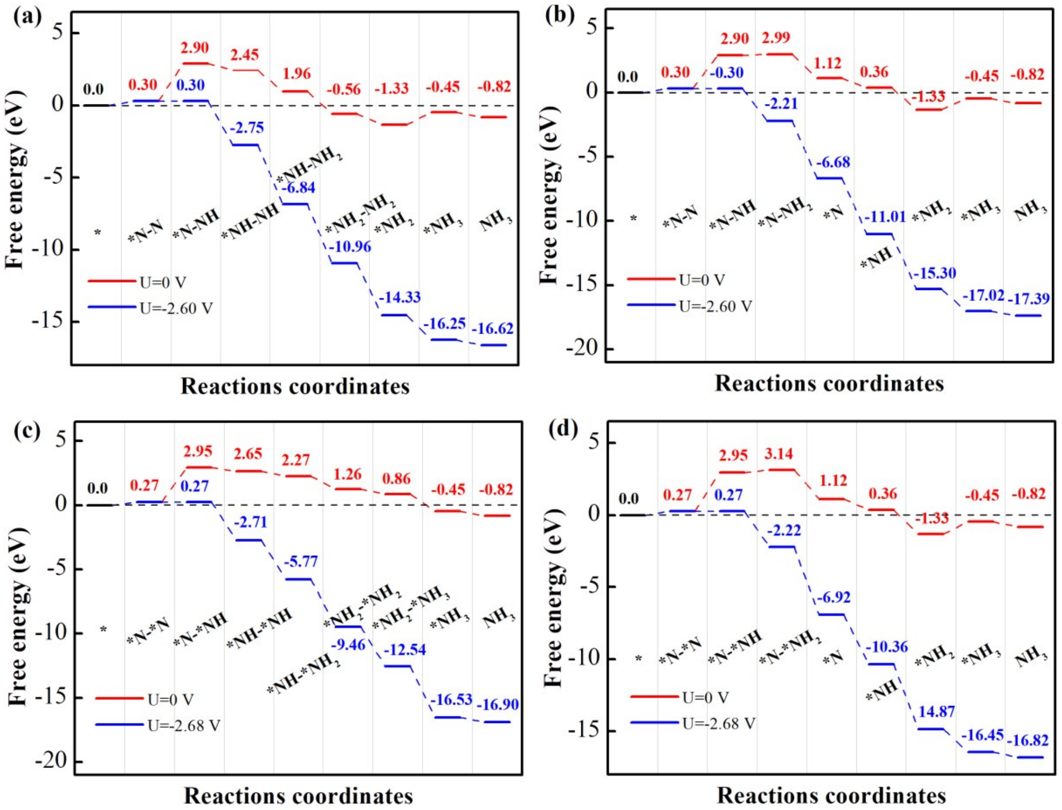

Figure S4. Free energy diagrams of NRR on Ti_2NO_2 surface through (a) alternating, (b) distal, (c) enzymatic, and (d) consecutive mechanisms under different applied potentials.

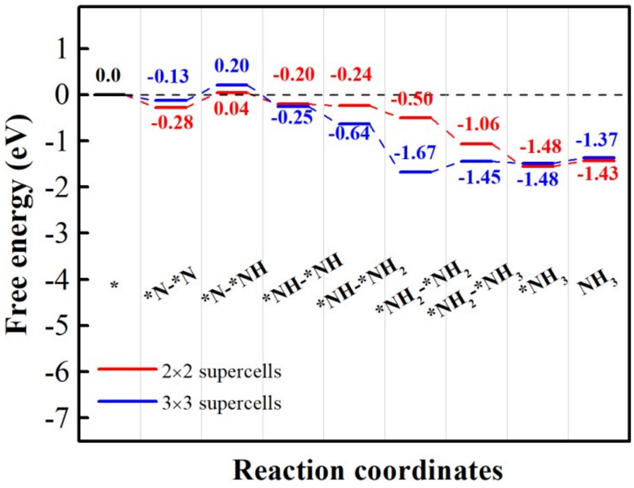

Figure S5. Reaction Gibbs free energy diagrams of NRR on Mo/Ti_2NO_2 through enzymatic, mechanism under 2×2 (red line) and 3×3 (blue line) supercell calculation models.

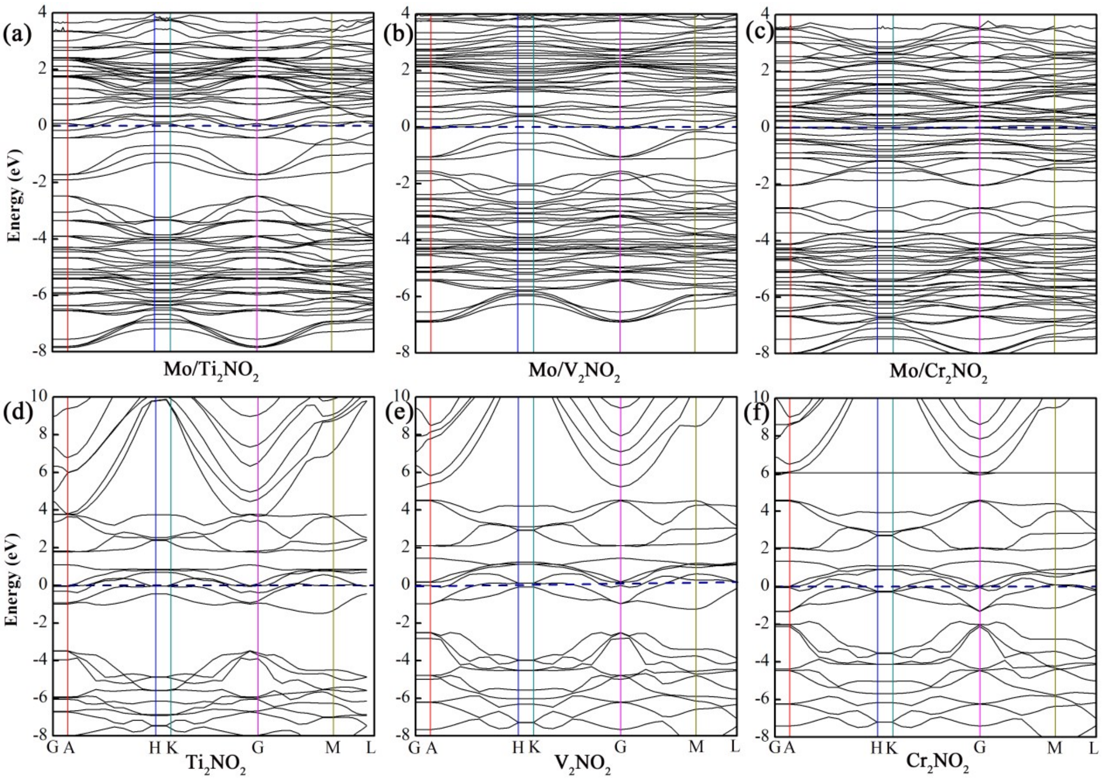

Figure S6. Band structures of M_2NO_2 (bottom) and Mo/M_2NO_2 (top) (M=Ti, V, and Cr).

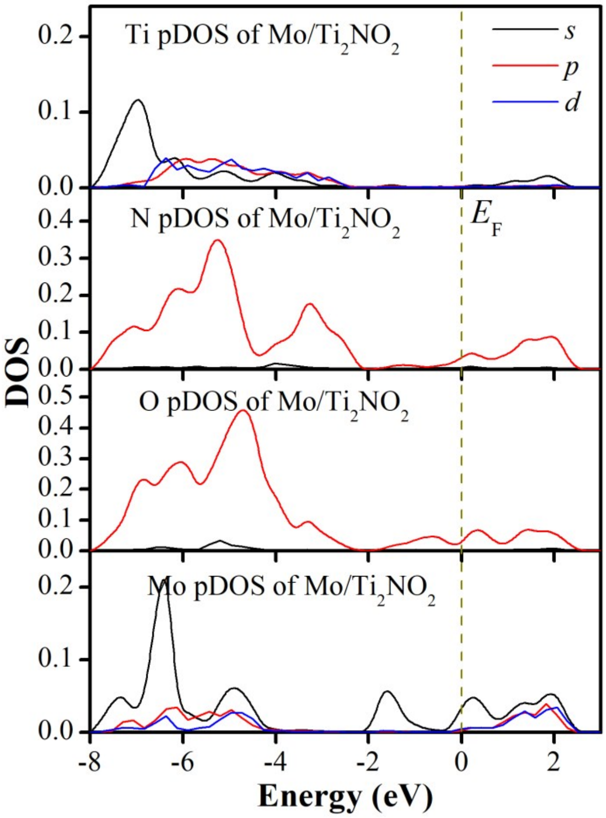

Figure S7. Partial densities of states of Ti, N, O, and Mo atoms of Mo/Ti_2NO_2.

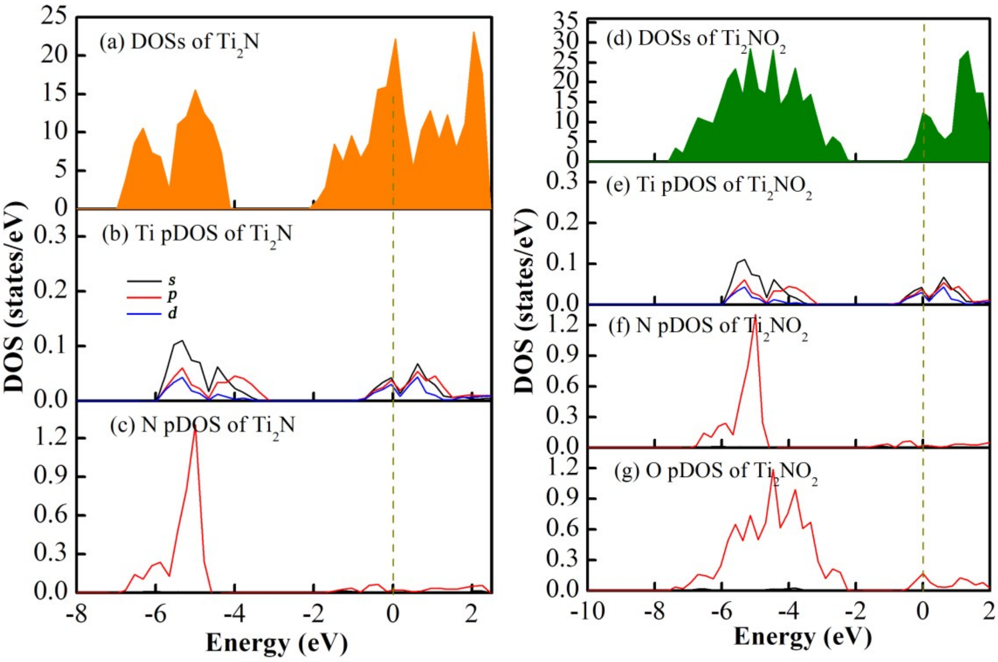

Figure S8. (a) DOSs of Ti_2N, (b) Ti pDOS of Ti_2N, (c) N pDOS of Ti_2N, (d) DOSs of Ti_2NO_2, (e) Ti pDOS of Ti_2NO_2, (f) N pDOS of Ti_2NO_2, and (g) O pDOS of Ti_2NO_2.

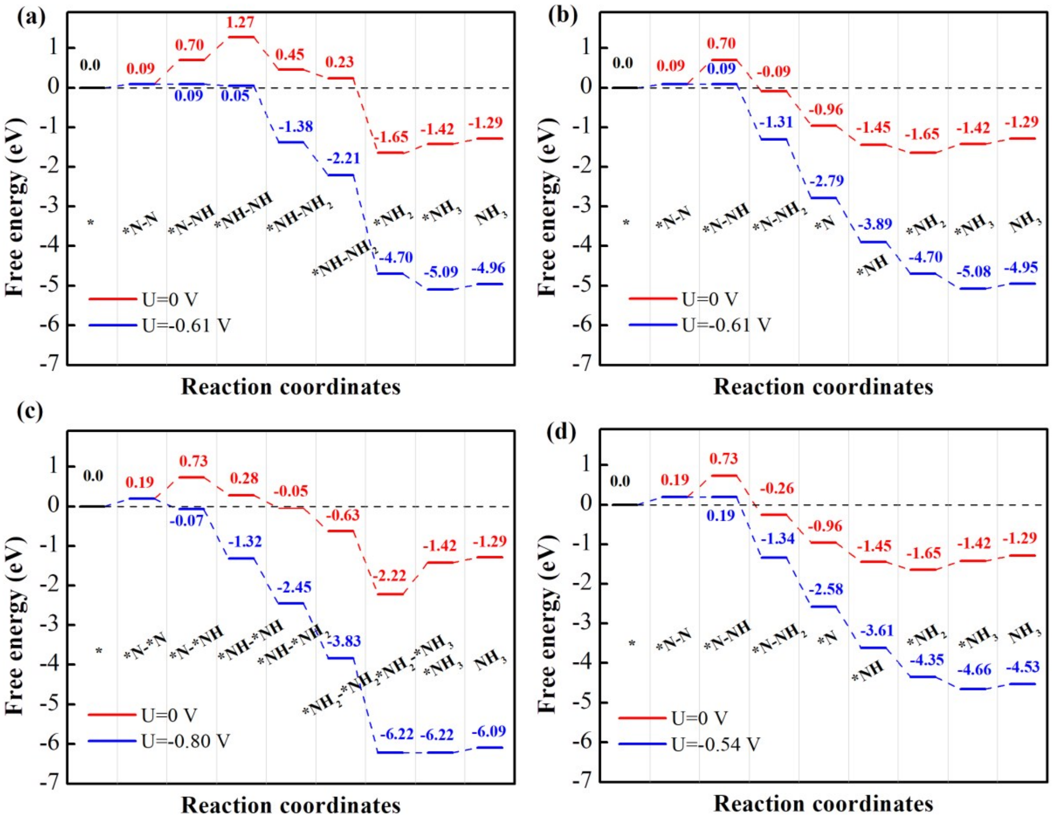

Figure S9. Free energy diagrams of NRR on Mo/V_2NO_2 through (a) alternating, (b) distal, (c) enzymatic, and (d) consecutive mechanisms under different applied potentials.

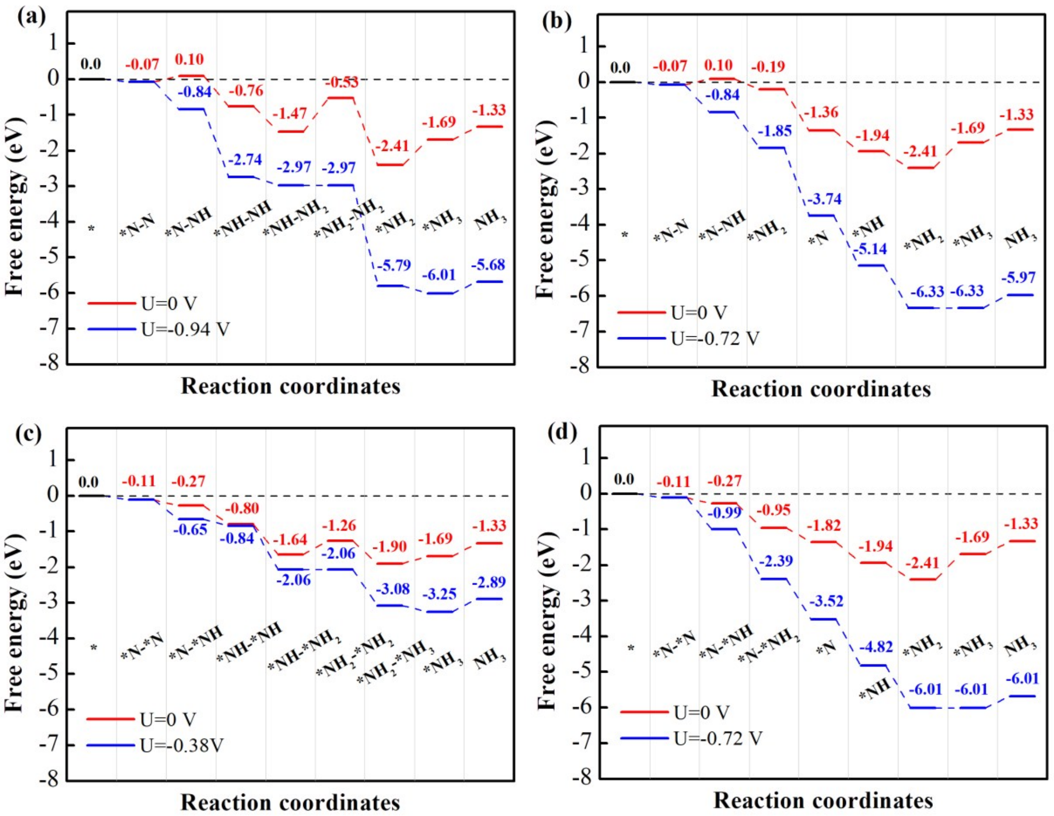

Figure S10. Free energy diagrams of NRR on Mo/Cr_2NO_2 through (a) alternating, (b) distal, (c) enzymatic, and (d) consecutive mechanisms under different applied potentials.

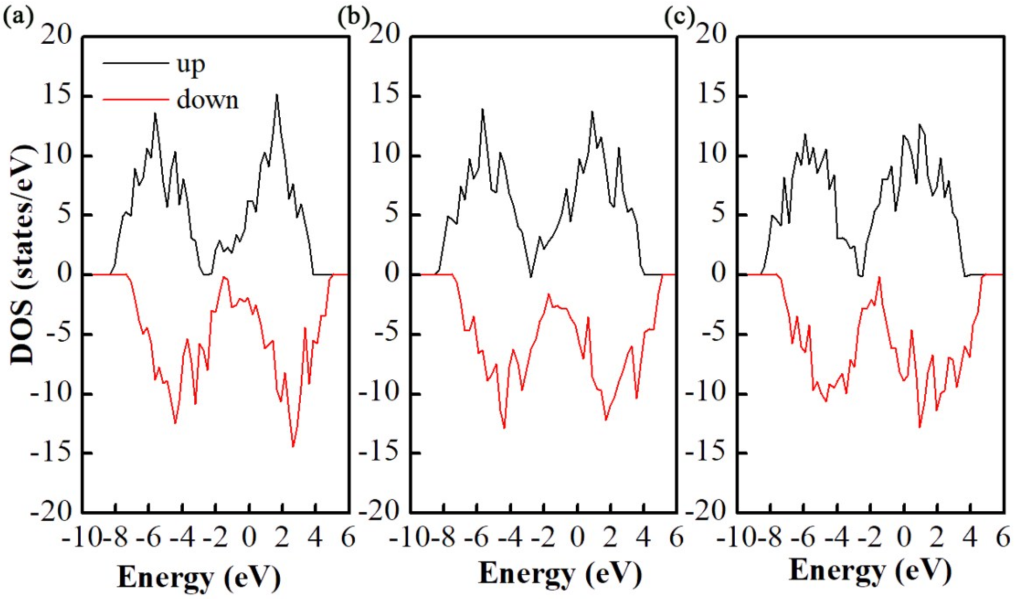

Figure S11. Densities of states of M_2NO_2 with considering spin- polarization, (a) Ti_2NO_2, (b) V_2NO_2, and (c) Cr_2NO_2.

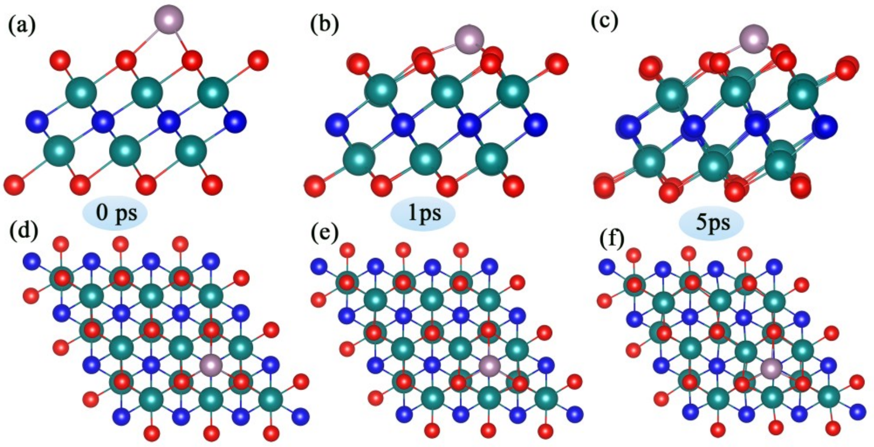

Figure S12. Atomic configurations of Mo/Ti_2NO_2 after a*b initio* molecular dynamics (AIMD) simulations under the temperature of 500K. The AIMD calculations were typically run for 1ps and 5ps, with a time step of 2fs. (a) 0ps, (b) 1ps, (c) 5ps, (d) 0 ps top view, (e) 1ps top view, and (f) 5ps top view.

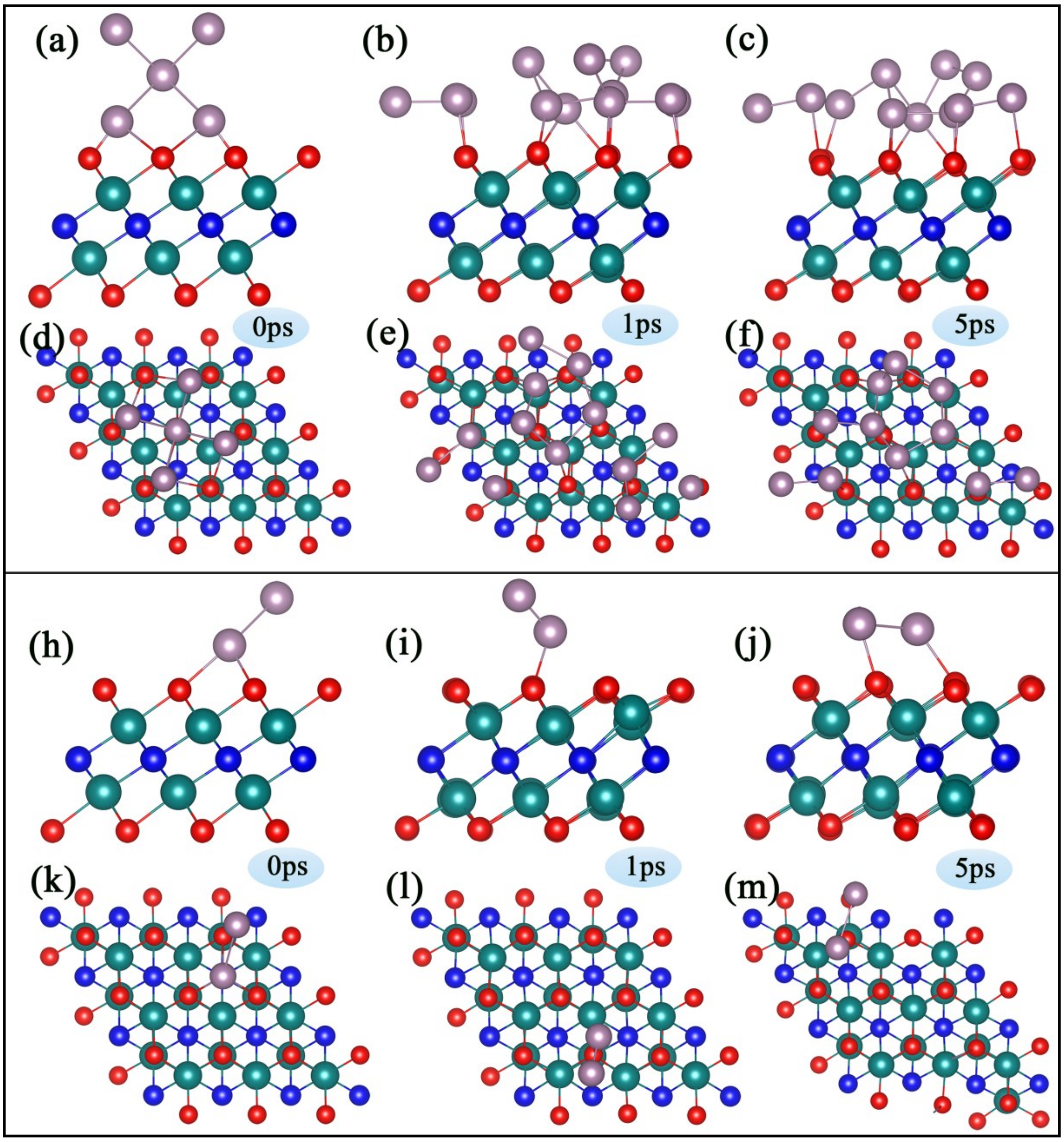

Figure S13. Atomic configurations of Mo_9/Ti_2NO_2 after AIMD simulations under the temperature of 500K (the top panel). The AIMD calculations were typically run for 1ps and 3ps, with a time step of 2fs. (a) 0ps, (b) 1ps, (c) 3ps, (d) 0 ps top view, (e) 1ps top view, and (f) 5ps top view. Atomic configurations of Mo$_2$/Ti$_2$NO$_2$ at end of AIMD simulations under the temperature of 500K (the bottom panel). The AIMD calculations were typically run for 1ps and 3ps, with a time step of 2fs. (h) 0ps, (i) 1ps, (j) 3ps, (k) 0 ps top view, (l) 1ps top view, and (m) 3ps top view.

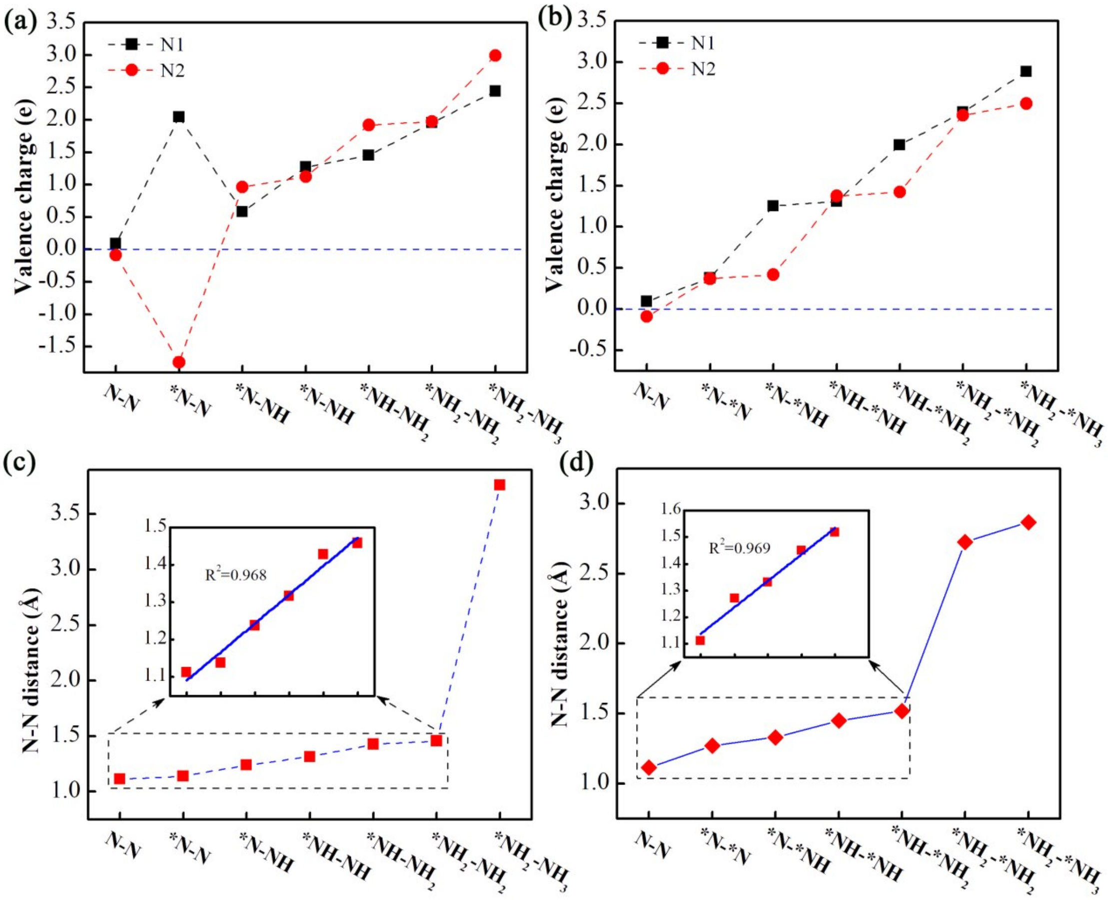

Figure S14. Valence charges of each intermediate during NRR on Mo/V$_2$NO$_2$ via the end-on (a) and side on (b) adsorptions, the N−N bond length of intermediate during NRR via end-on (c), and side-on (d) adsorptions, where the bond lengths increases linearly before N$_2$ is being broken.

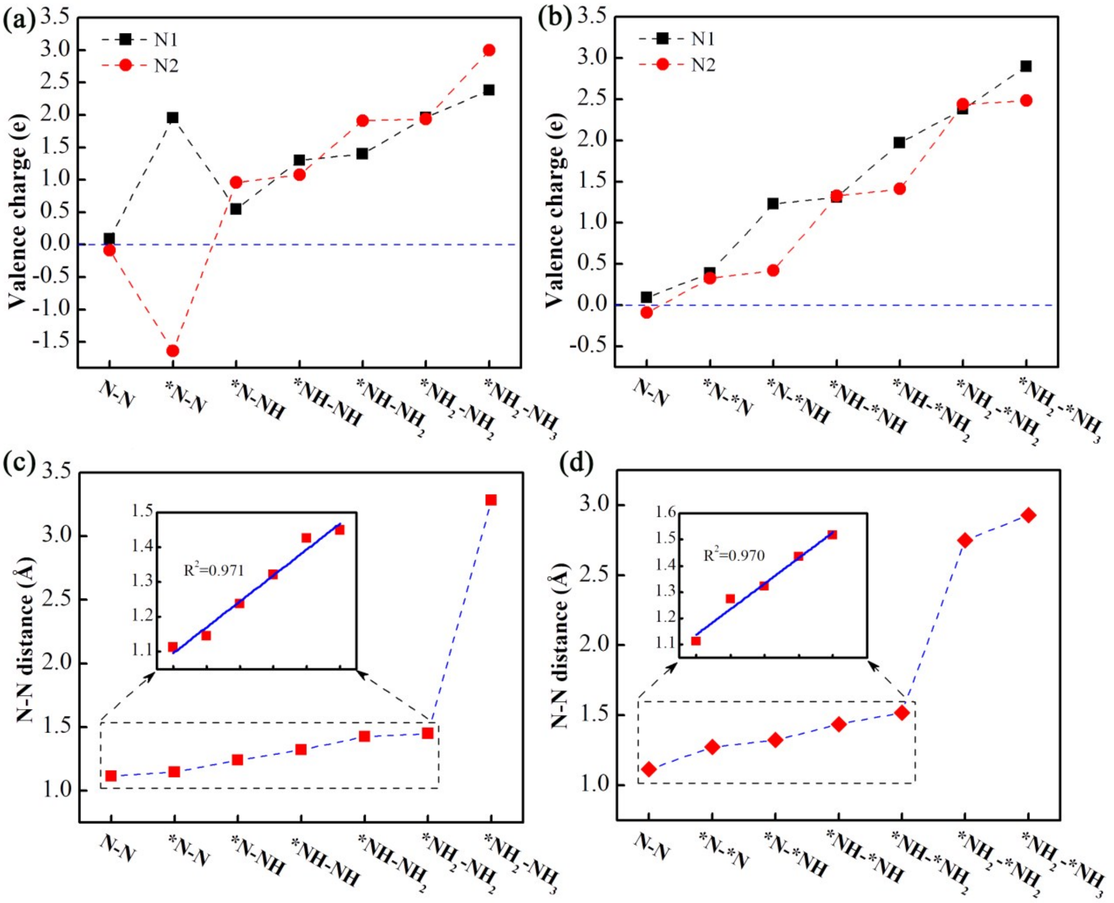

Figure S15. Valence charges of each intermediate during NRR on Mo/Cr_2NO_2 via the end-on (a) and side on (b) adsorptions, the N−N bond length of intermediate during NRR via end-on (c), and side-on (d) adsorptions, where the bond lengths increases linearly before N_2 is being broken.

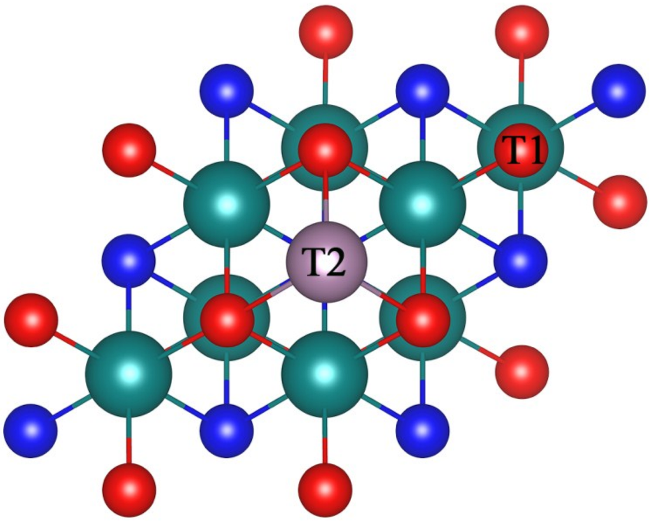

Figure S16. Schematic of hydrogen adsorptions on Mo/Ti_2NO_2 surface.

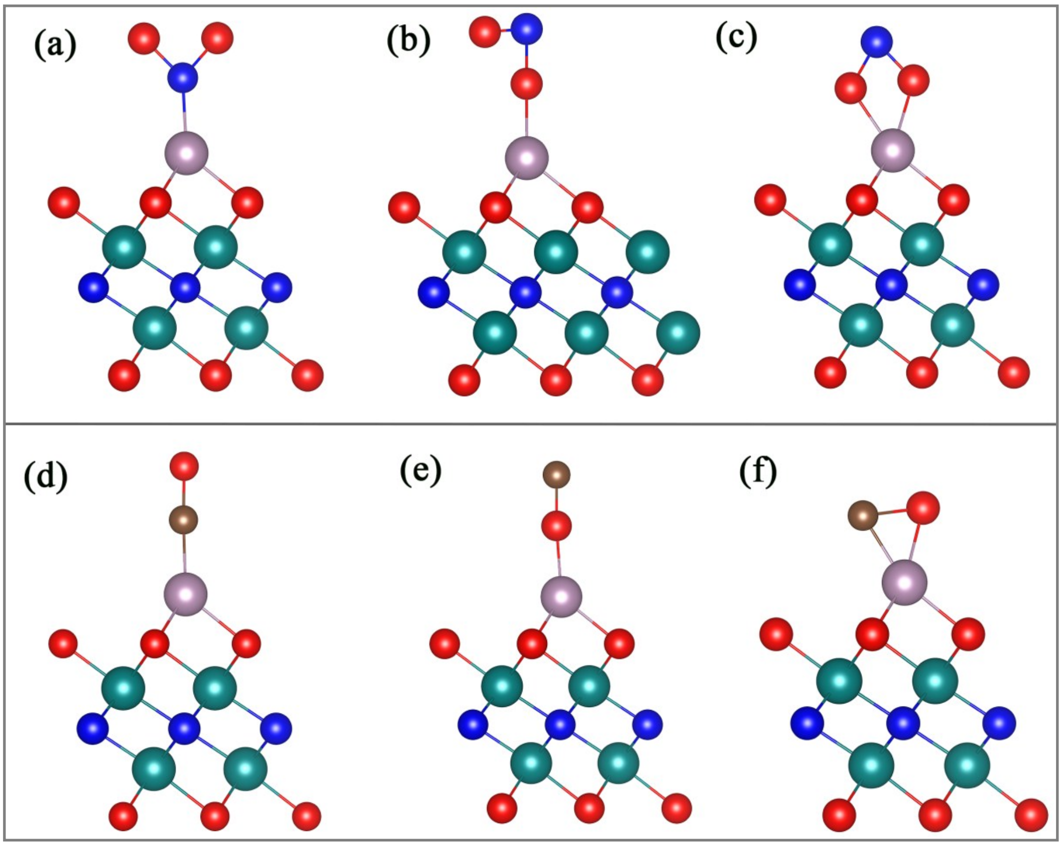

Figure S17. Schematic of gas molecule adsorptions on Mo/Ti_2NO_2 surface. (a) end-on mechanism of N interacting with catalyst for NO_2 adsorption, (b) end-on mechanism of O interacting with catalyst for NO_2 adsorption, (c) side-on mechanism of NO_2 adsorption, (d) end-on mechanism of C interacting with catalyst for CO adsorption, (e) end-on mechanism of O interacting with catalyst for CO adsorption, and (f) side on mechanism of CO adsorption.

Table S1. The lattice parameters of bulk M_2N, M_2NO_2, M_2NF_2 and $M_2N(OH)_2$ (M= Ti, V, and Cr) with *P*63/*mmc* symmetry.

M_2AC	a(Å)	c(Å)	c/a
Ti_2N	2.976	13.168	4.424
Ti_2NO_2	3.016	12.614	4.181
Ti_2NF_2	3.071	12.551	4.086
$Ti_2N(OH)_2$	3.004	10.576	3.521
V_2N	2.891	12.606	4.360
V_2NO_2	2.894	12.223	4.227
V_2NF_2	3.121	11.542	3.698
$V_2N(OH)_2$	3.005	10.189	3.391
Cr_2N	2.779	12.555	4.517
Cr_2NO_2	2.751	12.804	4.654
Cr_2NF_2	3.016	11.664	3.867
$Cr_2N(OH)_2$	3.457	11.177	3.233

Table S2. Total energies of 1×1 supercells of M_2NO_2, M_2NF_2 and $M_2N(OH)_2$ (M= Ti, V, and Cr).

systems	fcc (eV)	hcp (eV)	top (eV)
Ti_2NO_2	-42.558	-41.254	-25.473
Ti_2NF_2	-36.323	-36.086	-35.554
$Ti_2N(OH)_2$	-53.819	-53.567	-48.899
V_2NO_2	-39.201	-39.110	-27.746
V_2NF_2	-33.763	-33.491	-22.132
$V_2N(OH)_2$	-37.550	-35.382	-33.251
Cr_2NO_2	-35.858	-35.720	-20.904
Cr_2NF_2	-30.665	-30.287	-29.509
$Cr_2N(OH)_2$	-40.237	-28.541	-39.415

Table S3. Binding energies (E_b) of M_2NO_2, M_2NF_2 and $M_2N(OH)_2$ (M= Ti, V, and Cr).

systems	O* (eV)	F (eV)	OH (eV)
Ti_2NT_x	-5.923	-3.654	-4.119
V_2NO_2	-4.828	-2.961	2.431
Cr_2NO_2	-4.040	-2.293	0.205

Table S4. Relative energies of Ti_2NO_2 and TM/M_2NO_2 systems with TM anchored at H1, H2, and T1 sites, respectively.

Systems	H1 site (eV)	H2 site (eV)	T1 site (eV)
Mo/Ti_2NO_2	3.45	4.96	5.29
Mo/V_2NO_2	14.76	14.65	16.10
Mo/Cr_2NO_2	-6.64	-5.18	-2.63
Mn/Ti_2NO_2	-5.01	-4.27	-1.28
Fe/Ti_2NO_2	-3.82	-3.27	-1.94
Co/Ti_2NO_2	-2.81	-2.35	-0.51
Ni/Ti_2NO_2	-1.92	-1.79	-0.17
Cu/Ti_2NO_2	-0.49	-0.36	0.27

Table S5. Binding energies of TM with M_2NO_2.

Systems	Binding energy (eV)
Mo/Ti_2NO_2	-1.71
Mo/V_2NO_2	-0.98
Mo/V_2NO_2	-1.42
Mn/Ti_2NO_2	1.38
Co/Ti_2NO_2	1.70
Ni/Ti_2NO_2	0.14
Fe/Ti_2NO_2	1.45
Cu/Ti_2NO_2	2.38

Table S6. The Gibbs reaction free energies (eV) of intermediates ($\Delta G_{1\text{-}12}$) through alternating and distal mechanisms in TM/M_2NO_2 systems.

Systems	ΔG_1	ΔG_2	ΔG_3	ΔG_4	ΔG_5	ΔG_6	ΔG_7	ΔG_8	ΔG_9	ΔG_{10}	ΔG_{11}	ΔG_{12}
Mo/Ti_2NO_2	-0.32	0.58	0.54	-0.93	0.72	-2.47	0.33	0.12	-0.84	-0.79	-0.34	-0.17
Mo/V_2NO_2	0.09	0.61	0.57	-0.82	-0.22	-1.88	0.23	0.13	-0.79	-0.87	-0.49	-0.20
Mo/Cr_2NO_2	-0.07	0.17	-0.86	-0.71	0.94	-1.88	0.72	0.36	-0.29	-1.17	-0.57	-0.47
Mn/Ti_2NO_2	-0.75	0.55	0.64	0.05	-0.76	-1.74	0.75	0.50	-0.02	-0.71	-0.16	-0.62
Fe/Ti_2NO_2	-1.02	0.87	0.49	-0.14	-2.14	2.09	-1.11	0.93	0.34	2.99	-2.08	-2.33
Co/Ti_2NO_2	-1.05	1.03	0.43	0.30	-0.11	-1.47	-0.60	0.68	0.53	0.55	-0.57	1.06
Ni/Ti_2NO_2	2.09	-1.82	1.37	-0.38	-0.10	-1.31	-0.66	0.74	0.59	1.60	-1.78	-1.62
Cu/Ti_2NO_2	1.34	0.03	-0.51	0.20	-0.71	-0.99	-1.03	0.94	-0.33	3.04	-2.09	-2.60
Ti_2NO_2	0.30	2.60	-0.45	-1.49	-1.52	0.77	0.88	-0.37	0.09	1.87	-0.76	-1.69

Table S7. The Gibbs reaction free energies (eV) of intermediates ($\Delta G_{13\text{-}21}$) through enzymatic and consecutive mechanisms in TM/M_2NO_2 systems.

Systems	ΔG_{13}	ΔG_{14}	ΔG_{15}	ΔG_{16}	ΔG_{17}	ΔG_{18}	ΔG_{19}	ΔG_{20}	ΔG_{21}
Mo/Ti_2NO_2	-0.28	0.32	-0.24	-0.04	-0.26	-0.56	-0.49	-0.90	-0.51
Mo/V_2NO_2	0.19	0.54	-0.45	-0.33	-0.58	-1.02	0.80	-0.99	-0.70
Mo/Cr_2NO_2	-0.11	-0.16	-0.53	-0.84	0.38	-0.64	0.21	-0.68	-0.41
Mn/Ti_2NO_2	-0.35	0.55	-0.06	-2.10	-1.30	0.29	-0.88	-0.61	-0.49
Fe/Ti_2NO_2	-0.46	0.72	0.15	-0.56	-1.35	0.13	0.22	3.96	2.75
Co/Ti_2NO_2	-0.45	0.80	0.32	-0.61	-0.79	-1.08	0.33	0.13	1.06
Ni/Ti_2NO_2	-0.43	0.91	0.14	-0.50	-0.59	-1.42	0.22	0.54	1.35
Cu/Ti_2NO_2	-0.21	1.58	-.36	0.29	-0.81	-1.65	-0.64	-0.22	2.76
Ti_2NO_2	0.27	2.68	-0.30	-0.38	-1.01	-0.40	-1.31	0.19	-2.02

Table S8. The calculated η_{NRR} and electrons (based Bader charge analysis) of adsorbed N_2 receiving and TM losing of TM/Ti_2NO_2 systems.

Systems	η_{NRR} (V)	adsorbed N_2 receiving electrons (*e*)	TM losing electrons (*e*)
Mo/Ti_2NO_2	0.16	0.52	1.58
Mn/Ti_2NO_2	0.39	0.38	1.17
Fe/Ti_2NO_2	0.56	0.35	1.07
Co/Ti_2NO_2	0.64	0.30	0.96
Ni/Ti_2NO_2	0.75	0.27	0.91
Cu/Ti_2NO_2	1.42	0.19	0.87
Ti_2NO_2	2.44	-0.03	-

Table S9. The adsorption energies (eV) of adsorbed N_2 on Mo/M_2NO_2 surface via the end-on and side-on adsorptions.

Adsorption	Mo/Ti_2NO_2	Mo/V_2NO_2	Mo/Cr_2NO_2
End-on	-0.94	-0.36	-0.37
Side-on	-1.05	-0.28	-0.52

Table S10. Valence charge (in unit of *e*) variation of N atom in intermediates of NRR on Mo/M_2NO_2 surface via the end-on and side-on adsorption styles.

Adsorption	Adsorbed intermediates	Mo/Ti_2NO_2	Mo/V_2NO_2	Mo/Cr_2NO_2
End on	N_2	0.091, -0.091	0.091, -0.091	0.091, -0.091
	*N-N	0.711, -0.366	2.046, -1.746	1.955, -1.641
	*N-NH	0.581, 0.953	0.579, 0.961	0.547, 0.959
	*NH-NH	1.299, 1.076	1.273, 1.121	1.303, 1.074
	*NH-NH_2	1.429, 1.929	1.451, 1.922	1.397, 1.911
	*NH_2-NH_2	2.027, 2.012	1.955, 1.973	1.961, 1.935
	*NH_2-NH_3	2.435, 2.999	2.441, 2.993	2.381, 2.997
	*N-NH_2	0.699, 1.881	0.696, 1.861	0.698, 1.851
	*NH_3	2.943	2.921	2.931
Side on	N_2	0.091, -0.091	0.091, -0.091	0.091, -0.091
	*N-*N	0.323, 0.195	0.377, 0.368	0.391, 0.325
	*N-*NH	1.249, 0.441	1.254. 0.418	1.229, 0.421
	*HN-*NH	1.346, 1.339	1.309, 1.376	1.309, 1.326
	HN-NH_2	1.998, 1.427	1.993, 1.422	1.971, 1.412
	H_2N-NH_2	2.383, 2.406	2.394, 2.356	2.378, 2.439
	H_2N-NH_3	2.896, 2.501	2.885, 2.498	2.897, 2.482
	N-NH_2	1.979, 0.641	1.976, 0.627	1.956, 0.611
	*NH_3	2.943	2.921	2.931